# Effect of Excitation on Coaxial Jet Noise

H. Y. Lu*
*Boeing Commercial Airplane Company, Seattle, Washington*

**Coaxial model jets, including those of high bypass ratio engine exhaust hot gas conditions, were excited internally by tone and broadband noise. Acoustic excitation in the secondary (outer) duct was found to be most effective in jet noise amplification due to the sensitivity of the outer shear layer. Jet noise amplification at the subharmonic of the excitation frequency occurred in a number of cases. An acoustic elliptic mirror was used to observe the noise sources along the jet. It revealed local noise source characteristics in different shear layer regions and noise source location changes from unexcited to excited jets.**

## Nomenclature

$A$ = nozzle flow exit area
$AR$ = area ratio $= A_s/A_p$
$D$ = nozzle exit diameter
$D_j$ = reference jet diameter $= 2\sqrt{(A_s + A_p)/\pi}$
$f$ = frequency, Hz
$PR$ = nozzle pressure ratio
$S$ = Strouhal number $= fD_j/V_j$
$T_T$ = total temperature
V = jet velocity
$V_j$ = reference jet velocity, the greater of $V_p$ and $V_s$
$X$ = axial distance downstream from primary nozzle exit
$x$ = dimensionless distance $= X/D_j$
$\theta$ = angle relative to inlet axis, deg

*Subscripts*

$p$ = primary (inner) nozzle
$s$ = secondary (outer) nozzle

## Introduction

DETAILED analysis of noise components of several high bypass ratio (HBPR) engines has been conducted. Comparisons of engine jet noise component with scaled model jet noise data indicate relatively high levels for the engine jet noise, particularly at low power settings and at forward and normal angles. It is believed that jet noise amplification due to upstream acoustic excitation is the most probable cause of the relatively high jet noise level of the engine.

Jet broadband noise amplification (excess jet noise) was demonstrated by Gerend et al.[1] They tested coplanar, coaxial model jets at simulated HBPR engine gas conditions by noise injected into the primary (inner) flow. It was found that the resulting noise was in excess of the sum of the unexcited jet and internal noise. The noise amplification from single jets by tone excitation was investigated by Bechert and Pfizenmaier.[2] They found an order of 5 dB in excess jet noise. However, recent tests of Jubelin[3] found little or no excess jet noise for coaxial jets with primary flow excitations, whereas single jets with comparable excitations showed excess jet noise. The difference between the coaxial jet test results of Gerend et al. and Jubelin may represent the sensitivity of coaxial jet excess noise to hardware configuration and the specific primary internal noise excitations. This present study included an evaluation of the excess jet noise sensitivity to configuration changes.

Presented as Paper 81-2044 at the AIAA 7th Aeroacoustics Conference, Palo Alto, Calif., Oct. 5-7, 1981; submitted Oct. 16, 1981; revision received May 13, 1982. 

*Senior Specialist Engineer, Noise Research Unit.

A typical HBPR engine is known to have internal noise radiation out of both core (primary) and fan (secondary) nozzles. It is believed that the fan noise in the secondary (outer) duct may cause HBPR engine excess jet noise. Spectral analysis of HBPR engine noise indicates relatively high jet noise levels (humps) centered at the first and the second harmonics of fan shaft frequency. This is based on comparisons with extrapolated model clean jet noise. The difference is not totally due to the presence of fan noise. This suggests that in the jet noise dominated frequency range (50-200 Hz), the fan or the secondary internal noise excitation is more likely to be responsible for the HBPR engine excess jet noise. Since the effect of acoustic excitation in the secondary duct of coaxial jets was not investigated in previous tests, it was therefore emphasized in the present test. Primary internal acoustic excitations were included to observe the excess jet noise of coplanar and extended primary nozzle configurations.

It is important to investigate the characteristics and source locations of the excess jet noise for better understanding of the phenomenon and for application to jet noise prediction and extrapolation. Therefore a 1.5-m-diameter acoustic elliptic mirror system was used to observe the HBPR jet noise source characteristics and the noise source locations. The use of an elliptic mirror for local jet noise source investigation was demonstrated by Grosche et al.[4]

Finally, one of the objectives of this test was to improve prediction capability for HBPR engine jet noise. Emphasis was placed on the HBPR model tested at engine gas conditions. The model jet noise test results were also used to develop empirical predictions for jet noise, including excess jet noise, and compared with full scale engine data.

## Test Description

The test was conducted in the Boeing Anechoic Large Test Chamber. A schematic of test layout is shown in Fig. 1. Hardware used in the test included two primary and two secondary nozzles and the internal noise source system. A quiet dual-flow rig was used, where both streams included mufflers. Data were acquired by the acoustic elliptic mirror and acoustic data acquisition systems. A brief description of the special hardware used in this test is given below.

### Internal Noise Source System

An internal noise injection section (Fig. 1) was installed approximately 1.2 m upstream of the nozzle exit. The internal noise source system consisted of 16 Altec horn drivers rated at 50 W per driver. Eight drivers were wired in a series circuit for the primary and eight for the secondary. The drivers and both sides of the diaphragm were ventilated by a small amount of cold bleed air from the facility high pressure air supply. This ventilation served the dual purpose of equalizing the static

pressure on both sides of the diaphragm and cooling the driver system, particularly under hot gas flow conditions. Noise from the drivers was fed into the flow duct by the tube arrangement shown in Fig. 1. Tone or broadband noise were injected into the primary and secondary flows independently or simultaneously.

### Nozzle Configurations

Coaxial and single flow model nozzles were tested for jet noise with and without internal acoustic excitations. Three configurations, as shown schematically in Fig. 2, covered the HBPR case of area ratio 3.0 (configuration 1) and two low bypass ratio (LBPR) cases of area ratio 1.0 (configurations 2 and 3). The primary nozzle of configuration 2 was used for the single jet test. Coaxial jets of ambient temperature and heated gas conditions, including the current HBPR engine cycle exhaust conditions, were tested. Gas conditions were measured in the nozzle adapter section approximately 0.9 m upstream of the nozzle exit.

### Acoustic Measurements

Microphone arrays were located at 4.57- and 0.61-m sidelines as shown in Fig. 1. The 4.57-m sideline covered an angular range from 70 to 160 deg from primary nozzle exit relative to the inlet axis. The 0.61-m sideline covered from 50 to 168 deg.

A 1.5-m-diameter elliptic mirror was used to investigate the local jet noise source characteristics with and without acoustic excitations. The elliptic mirror has a major axis of 4 m and a distance of 3 m between two foci as shown in Fig. 1. The resolution of this elliptic mirror is approximately a 3-dB decrease in gain for a source dislocation of one wavelength from the far-focus across the mirror axis. The mirror was operated remotely from the control room for translational and rotational motions with the mirror far-focus always located on the jet axis. A microphone, for jet local noise measurement, was mounted at the near focal point 0.5 m from the mirror center surface. Stationary measurements and sweep recordings (at 2.54 cm/s) along the jet axis were taken from 0.3 m upstream to 2.74 m downstream of the primary nozzle exit station. As the elliptic mirror far-focus traverses along the jet axis, the SPL from the local noise sources at the far-focus is recorded by the elliptic mirror microphone located at the near-focus. The mirror angle between the inlet axis and the mirror axis remained constant during each axial sweep recording.

Rotational motion was remotely controlled to set the mirror at any angle from 60 to 140 degs between the mirror and the inlet axes. Each traverse recording was made for a given mirror angle, and four angles—60, 90, 120, and 140 deg—were chosen for observations. The mirror was on one side of the jet and the sideline microphones were on the other side. The mirror was stowed away in its upstream position to minimize the sound of reflection when the sideline microphones were taking data.

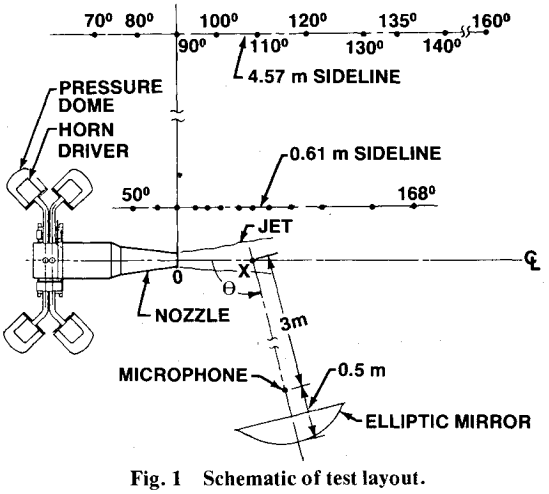


Fig. 1 Schematic of test layout.

### Control of the Acoustic Excitation

To set the most effective excitation frequency, an online FFT analyzer was used. First, the spectrum of the unexcited jet was acquired from a chosen microphone. Then, the internal tone excitation was turned on at its lowest frequency. Instantaneous (real-time) differences in SPL between the excited jet and the unexcited jet spectra were displayed by the analyzer so that the variation in excess jet noise was observed as the excitation frequency changed. Thus the excitation frequency that produces the most excess jet noise was determined for each gas condition. Extensive acoustic data were taken for the excited jet at the most effective excitation frequency.

For broadband noise excitation, a one-third octave band spectrum shaper was used. Broadband noise that simulates the core noise was chosen to excite the jet.

## Results

The jet noise amplification depends on a number of factors, such as nozzle configuration, gas condition, excitation frequency, excitation level and location, etc. The amplified jet noise or excess jet noise has a number of interesting characteristics that are presented and discussed in the following paragraphs.

### Local Noise Source Characteristics of HBPR Jets Without Excitation

In this section, the HBPR jets without internal acoustic excitation are examined by using the elliptic mirror. A

| CONF. NO. | PRI. $D_p$ (cm) | EXIT CONF. | SEC. $D_s$ (cm) | $A_s/A_p$ | SCHEMATIC SKETCH |
|---|---|---|---|---|---|
| 1 | 6.22 | 12.7 cm EXTENDED PRIMARY | 15.2 | 3.0 | |
| 2 | 8.79 | 12.7 cm EXTENDED PRIMARY | 15.2 | 1.0 | |
| 3 | 8.79 | COPLANAR | 12.4 | 1.0 | |

Fig. 2 Nozzle configurations.

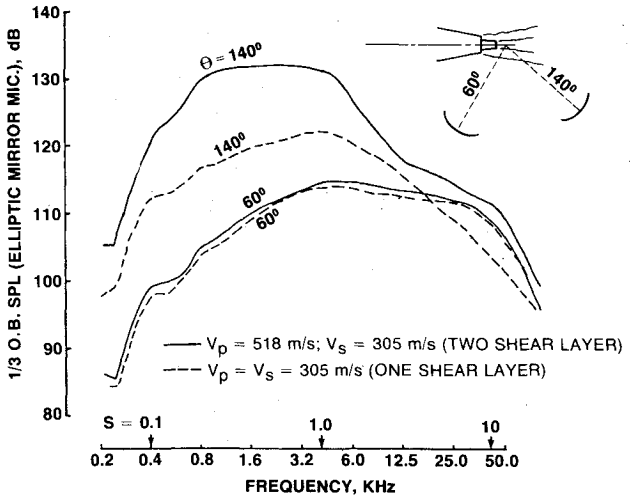


Fig. 3 Comparison of noise for two- and one-shear layer HBPR jets ($x = 1.22$).

knowledge of the local noise source characteristics of the HBPR jet premerged region (from nozzle exit to approximately 2 jet diameters downstream) is most useful in understanding the excess jet noise characteristics.

The HBPR model nozzle (configuration 1) was tested at a gas condition that has a primary jet velocity $V_p = 518$ m/s ($PR_p = 1.87$, $T_{Tp} = 811$ K) and a secondary jet velocity $V_s = 305$ m/s ($PR_s = 1.8$, $T_{Ts} = 298$ K). The premerged region of this coaxial jet has two shear layers: 1) the primary-secondary mixing shear layer, and 2) the secondary-ambient mixing shear layer. The same configuration was tested with primary gas condition identical to the secondary. Under this condition there is only one shear layer in the same premerged region which is the secondary-ambient mixing layer (wall boundary-layer wake is negligible). The spectra of the two jets from the elliptic mirror microphone are shown in Fig. 3. The mirror was focused at 15.2 cm ($x = 1.22$) downstream of the primary nozzle exit. When the mirror axis is at 60 deg relative to the inlet axis, very little difference in SPL exists between the two spectra, indicating that the inner shear layer does not radiate any dominating noise at this upstream angle. However, at 140 deg a large difference in SPL is shown in the spectra comparison. The inner shear layer at this location dominates the SPL in the downstream direction.

In order to see the differences in SPL at various locations and angles, the difference in one-third octave band SPL is plotted in Fig. 4 as ΔSPL between these two jets. One can see that between the primary nozzle exit ($x = 0$) to 30.5 cm ($x = 2.45$) downstream where the primary and secondary flows have not fully merged, the difference in SPL for 60 deg (upstream) and 90 deg (normal) mirror angles is less than 3 dB. This indicates that under this normal bypass gas condition (two shear layer) the primary-secondary premerged noise does not dominate the upstream and normal angles. However, at downstream angles, 120 and 140 deg, the difference in SPL exceeds 10 dB for some frequencies. Although the relative velocity between primary and secondary jets is 213 m/s, which is smaller than the relative velocity of 305 m/s between secondary and ambient, the primary-secondary mixing becomes a dominating noise source in the premerged region for downstream angles. The efficient noise radiation at downstream angles possibly is caused by the high convection velocity of turbulence in the primary-secondary mixing layer, which has an average velocity of approximately 427 m/s and is supersonic relative to ambient speed of sound.

To investigate the primary-secondary premerged noise, the same technique was applied to another gas condition. The secondary jet velocity in this case is 235 m/s and the primary jet velocity is 518 m/s. In this case, the primary-secondary relative velocity is greater than the secondary-ambient relative velocity, while the reverse is true in the previous case. As expected, the primary-secondary premerged jet noise dominates the total noise from the premerged region at all angles.

For all of the HBPR engines, the relative velocity between the primary and secondary is much smaller than that between the secondary and ambient. In this case, the secondary-ambient premerged jet noise dominates the upstream angles. This characteristic is closely related to the excess jet noise characteristics described in later sections.

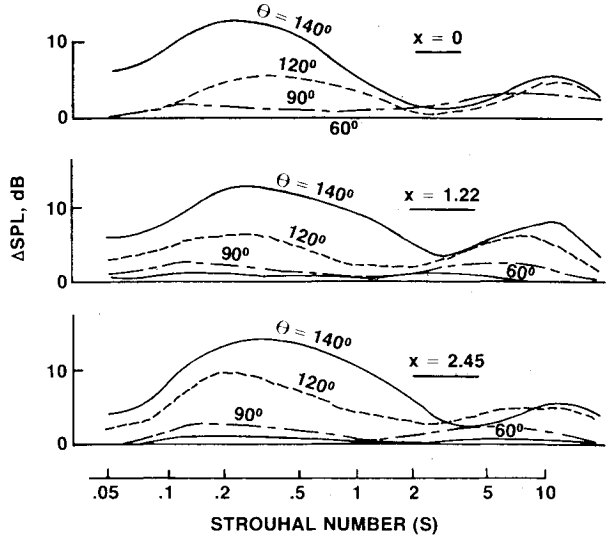


Fig. 4 Difference of local noise source spectra between two- and one-shear layer HBPR jets ($V_s/V_p = 0.59$).

### Jet Noise Amplification by Acoustic Excitation in Secondary Duct

The present experiment showed that the acoustic excitation in the secondary duct is effective in generating HBPR jet excess noise. An example of typical test results and analysis is given in this section.

Configuration 1 was tested at a gas condition that simulates the cutback condition of a HBPR engine. The secondary flow was excited at a frequency of 1600 Hz ($S = 0.53$). One-third octave band spectra with and without acoustic excitation are compared in Fig. 5 for a few selected angles. Strouhal number $S$ is shown along with the frequency scale for comparisons among different gas conditions or configurations. Broadband jet noise amplification occurred at all of the angles. The excitation tone appears in the 70-deg (forward arc) spectrum of jet with excitation. At higher angles, the jet broadband SPL increases and the tone becomes less noticeable. At 160 deg downstream the subharmonic (one-half of the tone frequency) can be identified in the excited jet noise spectrum. The amplification at the subharmonic also appears at 140 deg. An evaluation of jet noise amplification at the subharmonic of excitation frequency is described later.

The elliptic mirror was used to investigate the local noise source characteristics. Spectra from the elliptic mirror microphone are compared in Fig. 6a with the mirror at an angle of 120 deg and focused at the primary nozzle exit location ($x = 0$), which is 1.02 jet diameters downstream of the

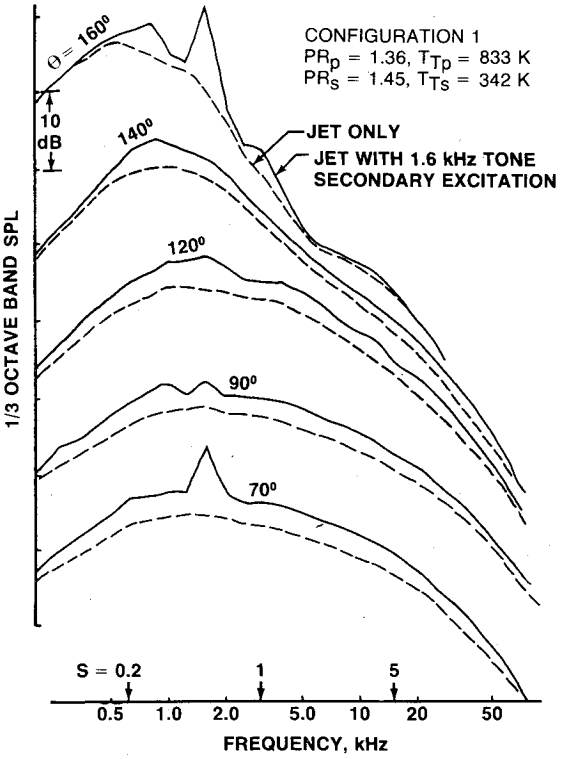


Fig. 5 HBPR jet noise spectra with and without acoustic excitation in secondary duct.

secondary nozzle exit. The comparison indicates some excess jet noise at low- to mid-frequencies ($S=0.3$ to 1.5) and essentially little or no amplification at high frequencies. The spectra at this location indicate a high level excitation tone. Comparison of spectra from the elliptic mirror microphone focused at 5 jet diameters downstream ($x=5$) is shown in Fig. 6b. The jet noise amplification at this location is about 5 dB in the measured frequency range. At this location, the spectrum of the jet with excitation does not display a tone at the excitation frequency, indicating that the excitation tone is mainly radiated from the nozzle exit and not distributed downstream.

The SPLs of the local noise sources along the jet axis as observed by the elliptic mirror are shown in Fig. 7 for a few selected frequencies (Strouhal numbers) at two directivity angles. It can be seen that for mid- to high frequencies ($S=1.32$ and 3.31), significant jet noise amplification occurs approximately in a region 2 to 6 jet diameters downstream of the nozzle exit. The amplification is relatively small close to the nozzle exit and in the region of 8 jet diameters downstream. It is believed that the excited jet mixes faster and the peak velocity decays faster than an unexcited jet. The crossover in SPL shown in Fig. 7 at downstream locations is an expected result. Low frequency (1000 Hz, $S=0.331$) excess noise occurs mainly in the first 6 jet diameters. The apparent amplification upstream of the secondary nozzle exit ($x=-1.02$) and far downstream ($x>14$) are due to the low resolution of the elliptic mirror for low frequency noise source location. It is interesting to compare the low frequency peak noise source locations shown in Fig. 7. The low frequency ($S=0.331$) peak SPL is located approximately at 8 jet diameters downstream of the unexcited jet (jet only). However, with excitation, the peak shifted to 5 jet diameters downstream. Again, this indicates that the excited jet mixes faster and the peak velocity decays faster than an unexcited jet.

The characteristics of excess jet noise caused by secondary excitation are described in the following few examples. For a given gas condition, the excess jet noise depends on excitation level and frequency.

The effect of internal noise excitation levels on the excess jet noise was tested on the HBPR model at a gas condition between an engine cutback and approach power. The internal noise excitation was adjusted to the highest level that the system can safely provide. The power input to the internal noise drivers was then reduced in steps of 3 dB. The excess jet noise in ΔdB is plotted against relative excitation input power in Fig. 8 for a few Strouhal numbers (frequencies). The ΔdB is the difference in SPL between the excited jet and the unexcited jet, while the input power is referred to the highest level of excitation. As the internal noise level reduces, the jet excess noise level reduces with it.

Broadband and tone excitations are compared in Fig. 9 for a simulated HBPR engine approach power gas condition. Excess jet noise from these two different excitations are comparable at all the measured angles. The relatively high level excess noise at the subharmonic of tone frequency can be easily identified in Fig. 9. The nearly equal excess jet noise in the mid- to high frequency ($S>2$) for two different types of excitation suggests that the broadband excess jet noise depends on jet flow condition rather than the detailed internal noise excitation spectrum. The excited jet noise spectra are similar to one another except in the region of excitation frequency and its subharmonic.

The excess jet noise directivity is plotted in Fig. 10 for a few Strouhal numbers. The excess jet noise level at excitation frequency should be considered differently from the rest. It represents the excitation tone with jet flow effects rather than the excess jet noise. It has been shown by elliptic mirror survey that the excitation tone is radiated at the nozzle exit while excess jet noise at other frequencies are located downstream. The excess jet noise changes very little from mid- to high frequency ($S=0.8$ to 5) and can be shown by a narrow region in Fig. 10. The excess jet noise decreases as the angle increases from upstream to downstream direction. This characteristic is closely related to the secondary-ambient premerged jet noise described earlier. It indicates that the outer shear layer is the origin of excess jet noise.

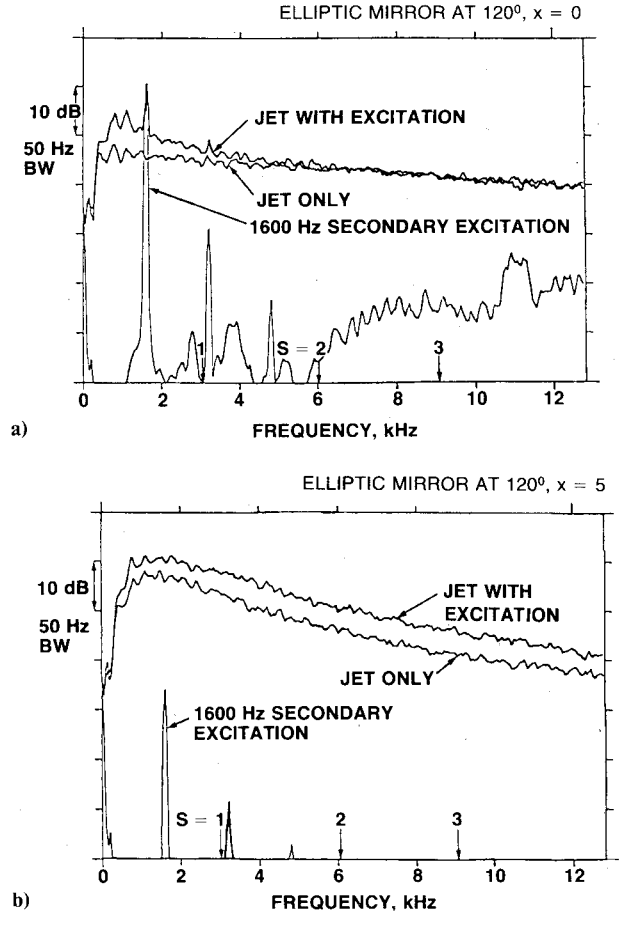


Fig. 6 HBPR jet local noise amplification.

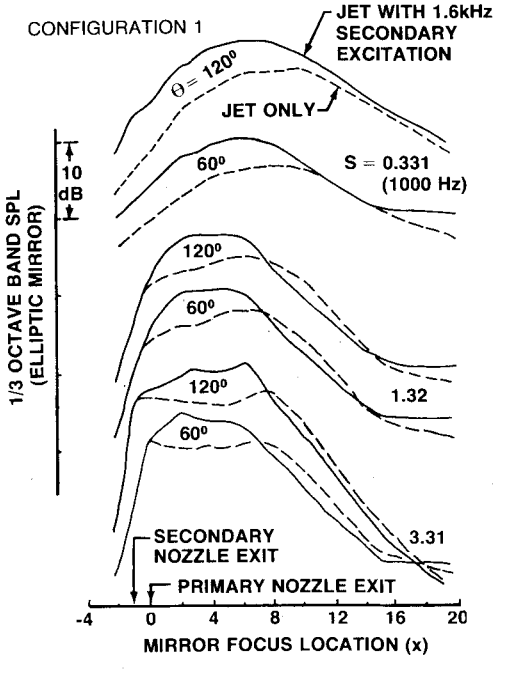


Fig. 7 HBPR jet local noise source SPL distributions.

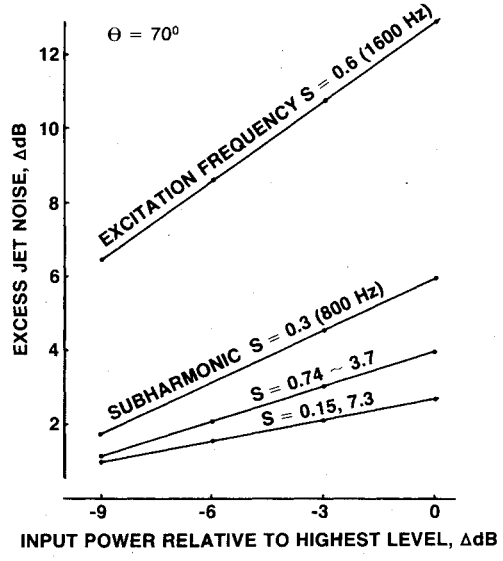


Fig. 8 Excess jet noise at different internal excitation levels.

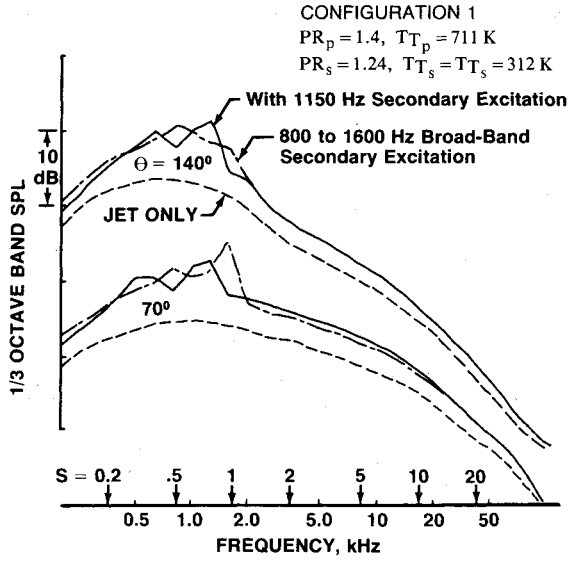


Fig. 9 HBPR jet noise amplification by single tone or broadband acoustic excitation in secondary duct.

The HBPR model (configuration 1) was also tested at cold flow gas conditions. In general, more excess jet noise can be obtained by excitation of cold flow than hot flow under comparable pressure ratios. At a primary pressure ratio of 1.8 the excess jet noise for the cold jet is approximately 2 to 3 dB at normal angles. On the other hand, little or no excess jet noise was observed for hot jets at this pressure ratio by either tone or broadband excitations.

#### Jet Noise Amplification by Acoustic Excitation in Primary Duct

Noise injection into the primary duct was tested for configurations 1 and 2 with extended primary nozzle exit. Jet noise amplification from primary excitation was of the order of 1 dB or less. This observation is in agreement with that of Jubelin.[3] Configuration 3 has the same primary and secondary exit areas as configuration 2 but with a coplanar exit. More excess jet noise (approximately 3 dB) due to primary excitation was found for this configuration than for the extended primary configuration. This observation and the more efficient secondary excitation indicate that the shear layer near the secondary (outer) nozzle lip is sensitive to excitation. For an extended primary configuration, acoustic excitation radiated from the primary exit interacts with a relatively thicker secondary-ambient shear layer as compared to a coplanar exit case. The acoustic excitation from the primary exit of the coplanar configuration is close to the relatively thin secondary-ambient shear layer at the secondary nozzle lip. It is believed that this initial stage of the outer shear layer is most important in the development of excess jet noise for the next few jet diameters. Excitation in the secondary duct is effective because the excitation interacts with the thin shear layer at the lip region.

#### Excess Jet Noise at the Subharmonic of Excitation Frequency

It has been mentioned in the previous cases of HBPR jets that relatively high level excess jet noise can occur at the subharmonic of excitation frequency. This phenomenon becomes outstanding for an LBPR model (configuration 2) jet under a gas condition where the primary and the secondary have the same total pressure and same total temperature. Acoustic excitation at 2850 Hz was injected into the secondary duct only. A narrowband spectra comparison in Fig. 11 clearly shows the tone and its harmonics. The amplification at subharmonic is almost broadband in nature as compared to a tone.

The elliptic mirror was used to observe the local noise source SPL. A comparison with and without excitation is shown in Fig. 12 for a few selected frequencies. The amplification occurs in a region from nozzle exit to several jet diameters downstream. The excitation tone is radiated from the secondary exit ($x = -1.02$) as expected. The apparent amplification downstream of 10 jet diameters ($x > 10$) is caused by the elliptic mirror gain directivity and is not real

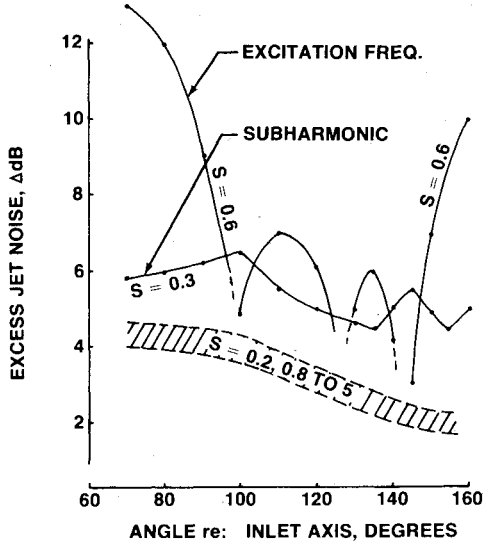


Fig. 10 Directivity of HBPR jet excess noise.

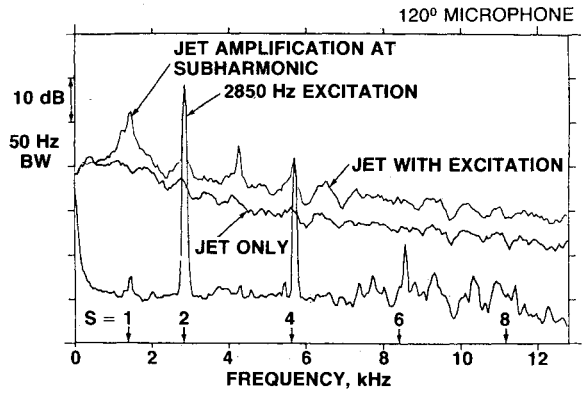


Fig. 11 Jet noise amplification at subharmonic of excitation frequency.

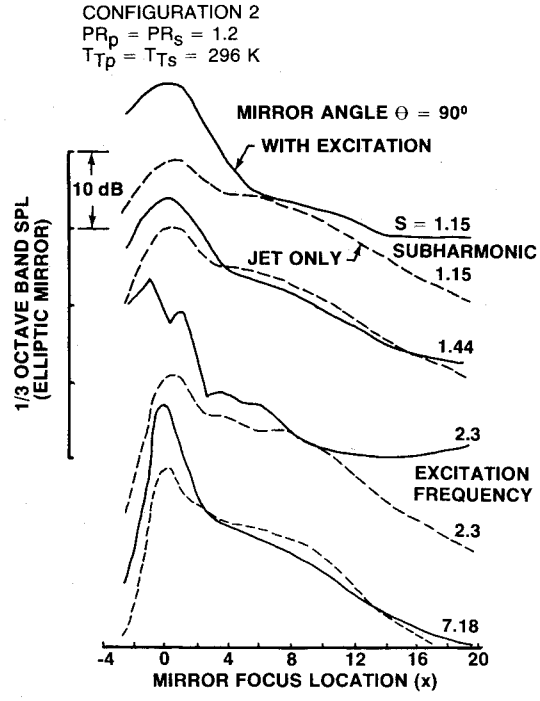


**Fig. 12 Local jet noise distribution showing amplification at the subharmonic of excitation frequency.**

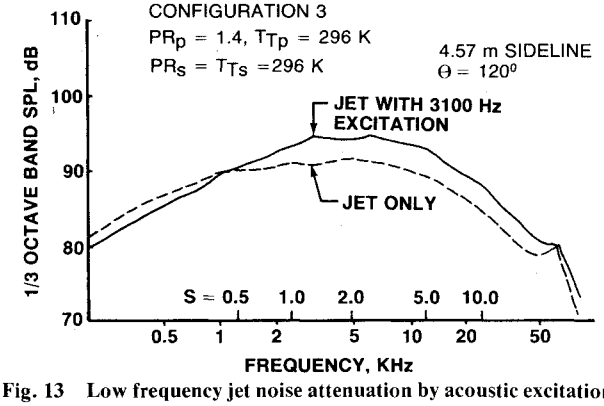


**Fig. 13 Low frequency jet noise attenuation by acoustic excitation.**

amplification. The amplification at subharmonic of excitation was observed by Jubelin[3] to occur only for single hot jets at downstream angles. However, in the present test for coaxial jets with secondary flow internal excitations, the subharmonic amplification was observed at both upstream and downstream angles, as shown in Fig. 9, and for both hot and cold jets. At downstream angles, the subharmonic amplification becomes very important for HBPR jets since it occurs at the peak SPL in the one-third octave band spectra (Fig. 5). The high level of subharmonic excess noise is probably due to the existence of vortex pairing[5-7] in a region where the amplification at subharmonic occurs. Measurements of flow and turbulence spectra[8] for relatively low velocity jets from the same nozzles confirmed that the vortex pairing is one of the mechanisms in generating excess jet noise.

#### Low Frequency Jet Noise Attenuation by Acoustic Excitation

A LBPR model (configuration 3) of coplanar exit was tested at a gas condition having an inverted velocity profile ($V_s > V_p$). Noise attenuation occurred at low frequencies as shown by spectra comparison in Fig. 13 with a relatively high frequency excitation in the secondary duct. The low frequency jet noise attenuation occurs also at other cold inverted velocity profile conditions. No hot flow inverted velocity profiles were tested for acoustic excitations. For hot bypass jets with normal velocity profiles the low frequency SPL usually increases due to acoustic excitations. However, a small amount (1 dB) of low frequency noise attenuation was observed at angles close to the jet axis.

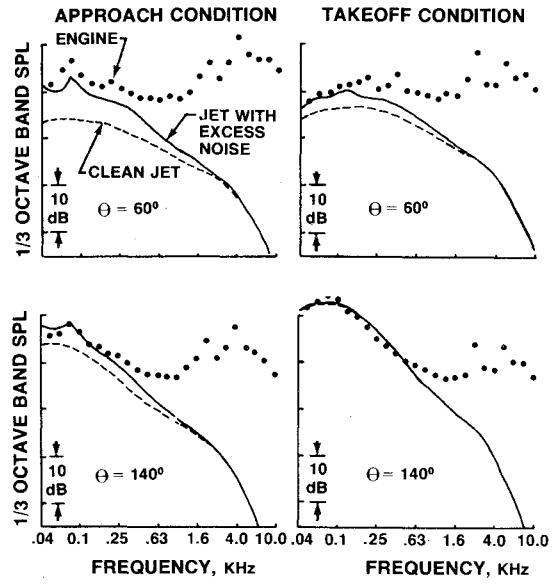


**Fig. 14 Comparison of engine data and empirical extrapolation.**

#### Acoustic Excitation of Single Jets

Single jets were also tested with and without acoustic excitations to compare results with those of coaxial flow cases. Results, in general, indicate that excitation of single jets is more efficient than coaxial jets with primary excitation (at comparable primary gas conditions), but less efficient than coaxial jets with secondary excitation.

## Comparison with HBPR Engine Jet Noise

Observed phenomena from this model test show a number of similarities between the model excess jet noise and engine jet noise characteristics by comparing engine data with the clean, model jet noise results. The excess jet noise test results and the clean model jet data were empirically extrapolated and are compared with HBPR engine data in Fig. 14. Comparisons should be limited to jet noise region (<200 Hz). At frequencies above 200 Hz, the engine noise is dominated by core and fan noise which should not be compared with the jet noise prediction. Improvement in agreement is clearly shown in the comparison when the excess noise model is used.

## Conclusions

The coaxial model jets with both secondary and primary excitations were tested for excess jet noise. The noise source regions were observed by using an elliptic mirror. Analysis of results provided a number of new findings that are summarized below.

1) Either tones or broadband acoustic excitation in the secondary (outer) duct of a coaxial jet can generate significant excess jet noise.

2) For primary (inner) duct excitations, modest excess jet noise was observed for coplanar exit configuration but little for extended primary configurations. This observation combined with the effective secondary excitation suggests that the secondary-ambient shear layer at the nozzle lip region is most sensitive to acoustic excitation.

3) Due to the increased mixing and higher noise level of the excited jet, the noise source region is more compact and the location is shifted relatively upstream as compared to the unexcited jet.

4) Excitation frequency with Strouhal numbers of 0.5 to 0.6 is found to be most effective in generating excess jet noise.

5) The relatively high level excess jet noise at the subharmonic of excitation frequency, probably due to vortex pairing, is important in that it occurs at or close to the peak SPL.

6) Single jets are easier to excite than coaxial jets with primary excitation. However, coaxial jets with secondary excitation generate the most excess jet noise.

7) More excess jet noise occurs in the forward arc than in the aft arc. The excess jet noise increases with increasing excitation level.

8) Comparison of the excess jet noise characteristics with HBPR engine jet noise data indicates that HBPR engines have excess jet noise.

## References

[1]Gerend, R. P., Kumasaka, H. A., and Roundhill, J. P., "Core Engine Noise," AIAA *Progress in Astronautics and Aeronautics, Aeroacoustics: Jet and Combustion Noise; Duct Acoustics*, Vol. 37, edited by H. T. Nagamatsu, MIT Press, Cambridge, Mass., 1975, pp. 305-326.

[2]Bechert, D. and Pfizenmaier, E., "On the Amplification of Broadband Jet Noise by a Pure Tone Excitation," AIAA Paper 76-489, June 1976.

[3]Jubelin, B., "New Experimental Studies on Jet Noise Amplification," AIAA Paper 80-0961, June 1980.

[4]Grosche, F.-R., Jones, J. H., and Wilhold, G. A., "Measurement of the Distribution of Sound Source Intensities in Turbulent Jets," AIAA *Progress in Astronautics and Aeronautics, Aeroacoustics: Jet and Combustion Noise; Duct Acoustics*, Vol. 37, edited by H. T. Nagamatsu, MIT Press, Cambridge, Mass., 1975, pp. 305-326.

[5]Moore, C. J., "The Role of Shear-Layer Instability Waves in Jet Exhaust Noise," *Journal of Fluid Mechanics*, Vol. 80, Pt. 2, 1977, pp. 321-367.

[6]Ffowcs Williams, J. E. and Kempton, A. J., "The Noise from the Large-Scale Structure of a Jet," *Journal of Fluid Mechanics*, Vol. 81, Pt. 4, 1978, pp. 637-694.

[7]Kibens, V., "Discrete Noise Spectrum Generated by an Acoustically Excited Jet," AIAA Paper 79-0592, March 1979.

[8]Berman, C. H., "Turbulence and Noise Characteristics of Acoustically Excited Bypass Jet Flows," AIAA Paper 81-2009, Oct. 1981.